

Nephroprotective effect of bone marrow mesenchymal stem cells on cisplatin induced kidney injury in albino rats

Mohamed Elsheikh¹, Heba A. Mubarak², Sayed Anwar Sayed³

¹ Department of Human Anatomy and Embryology, Faculty of Medicine, Aswan University, Aswan, Egypt

² Department of Histology and Cell Biology, Faculty of Medicine, Assiut University, Assiut, Egypt

³ Department of Human Anatomy and Embryology, Faculty of Medicine, Assiut University, Assiut, Egypt

SUMMARY

Cisplatin is a chemotherapeutic drug used in the treatment of a variety of cancers, with a known side effect of nephrotoxicity. Using stem cell therapy represents a distinctive and encouraging approach to remediate damaged organs. The administration of bone marrow mesenchymal stem cells (BMMSCs) has the potential to mitigate the adverse effects of cisplatin nephrotoxicity, thus helping with both functional and histological recuperation. Twenty-four mature male albino rats were divided into four groups. 1 ml of normal saline was injected intraperitoneally (I.P.) into the control group. Cisplatin was injected once (6 mg/kg I.P.) into the cisplatin group. 0.5 ml of culture media with 5×10^6 BMMSCs was injected i.p. with 6 mg/kg I.P. cisplatin in the BMMSC group. The withdrawal group received no treatment after cisplatin injections. At different times, groups were sacrificed. Kidney specimens were made for histology and immunohistochemistry. Morphometric and statistical studies were done. Blood urea and serum creatinine were evaluated before sacrifice. There were statistically significant differences between the studied groups regarding

markers of incidence of acute tubular necrosis and recovery, suggesting that cisplatin therapy caused acute tubular necrosis, whereas BMMSCs improved renal function markers, including blood urea and serum creatinine levels and tissue restoration. Stem cell rats also showed cluster of differentiation 44 (CD44) in cells near tubules, helping injured kidneys regenerate tubular cells. The use of bone-marrow-derived mesenchymal stem cells (BMMSCs) mitigated the nephrotoxic effects of cisplatin, thus showing a restorative effect on both functional and histological parts.

Key words: Cisplatin – Kidney – MSCs – CD44 – PCNA

INTRODUCTION

The symptoms of acute kidney injury (AKI) include an abrupt drop in glomerular filtration rate, the kidney's failure to eliminate wastes such as nitrogenous wastes, and disruption of the homeostasis of fluids and electrolytes. Drug-induced nephrotoxicity, in which the proximal convoluted tubules of the nephron are the major site of dam-

Corresponding author:

Mohamed Elsheikh, MD. Anatomy department, Faculty of Medicine, Aswan University, Aswan, 81528 Egypt. Phone: 00201008048586. E-mail: Melsheikh4047@gmail.com

Submitted: June 2, 2023. Accepted: September 22, 2023

<https://doi.org/10.52083/UFPK9237>

age, is one of the renal or intrinsic AKI causes (Makris and Spanou, 2016). Treatments for uraemic symptoms, electrolyte imbalance correction and pH issues, and fluid management are all part of the therapy for AKI; however, these treatments do not reverse the progressive irreversible decline in renal function (Fall and Szerlip, 2010). To find a permanent cure for kidney damage, it is imperative to investigate novel, non-traditional treatments for nephropathic patients. Cisplatin, also known as Cis-diamminedichloroplatinum (II), (CDDP), is an antineoplastic medication used to treat a variety of malignancies (Miller et al., 2010). There have been several hypothesized theories on how cisplatin causes nephrotoxicity, such as direct toxicity to renal tubular epithelial cells (McSweeney et al., 2021). A novel and promising therapeutic strategy for organ repair is stem-cell-based treatment (Aly, 2020). Bone marrow contains multipotent cells called MSCs that can develop into adipocytes, chondrocytes, and osteocytes (Ullah et al., 2015). MSCs are known to secrete soluble substances that aid damaged renal cells in healing (Du et al., 2013). According to certain studies, markers of renal cell activation and proliferation, such as immunostaining for PCNA in renal tissue, may be helpful in the diagnosis and/or prognosis of renal disorders (Pramanik et al., 2019). The advancement of renal disease may be linked to the rise in proliferating cell nuclear antigen (PCNA) expressions by renal cells (Pramanik et al., 2019). Moreover, PCNA participates in DNA repair, and its expression promotes the recovery of injured cells as well as mitogenesis and the replacement of depleted epithelial cells that results from it (Choe and Moldovan, 2017). Caspases (cysteine proteases) play a crucial role in the regulation and execution of apoptotic cell death and act upstream of DNA fragmentation (Yuan et al., 2016). A transmembrane adhesion glycoprotein called Cluster of Differentiation 44 (CD44) is essential for cell adhesion, motility, and inflammation (Senbanjo and Chellaiah et al., 2017). For the potential stem cells that may migrate inside the glomerular parietal epithelial cells of the adult kidney, CD44 has been recommended as a marker (Herrera et al., 2007). This study's objective was to determine if bone-marrow-derived stem cells can diminish the acute kidney injury (AKI) that cisplatin causes in Albino rats.

MATERIALS AND METHODS

Animals

Experimental group size: The sample size was calculated using G*Power program with α . Error = 0.05 and power 80% then the calculated sample size was 24 rats.

Rats were purchased from animal house. The experiment was done according to the guidelines of laboratory animals' care. Rats were divided into six in each cage, and were kept under a controlled housing condition with temperature $22^{\circ}\text{C} \pm 1^{\circ}\text{C}$, humidity $60\% \pm 10$ in an adequately ventilated room under a regular 12 h light/12h dark cycle. Free access to food and water ad libitum for 14 days before and during the experiment was provided. Rats weighing 180 to 220 grams were used in the present study.

Grouping: Rats were divided into four groups:

- Group I: the control group, which included 6 rats, received a single injection of 1 ml of normal saline intraperitoneal (I.P).
- Group II: the cisplatin-treated group, which included 6 rats, received a single injection of the drug (6 mg/kg I.P) dissolved in 1 ml of saline.
- Group III (n=6): this group included 6 rats, and received an intraperitoneal injection of 0.5 ml of culture media containing 5×10^6 BMMSCs and a single injection of Cisplatin (6 mg/kg I.P) dissolved in 1 ml of saline.
- Group IV: known as the withdrawal group, it included 6 rats that were not given any further therapy after receiving a cisplatin injection.

Rat sacrifice: The rats were anesthetized with a combination of xylazine (10 mg/kg, CEVA Santé Animale, Naaldwijk, the Netherlands) and ketamine (10 mg/kg, Ketaset®, Eurovet Animal Health, Bladel, the Netherlands) administered via intraperitoneal (i.p.) injections. Blood and bone marrow samples were then obtained.

Sample analysis: Eight days following injection, the control (group I) and cisplatin (group II) rats were sacrificed. One month later, the rats from both the cisplatin and bone-marrow stem-cell

treatment group (group III) and the withdrawal group (group IV) were slaughtered. There were visible kidneys, and following a mid-dorsal plane cut, the kidneys were removed and immediately fixed in 10% neutral formalin. Tap water was used to wash the tissue. In observance of Charmi et al. (2009), the paraffin sections were produced and stained with hematoxylin and eosin stain, and Masson trichrome stain for histological analysis.

Immunohistochemical technique

Paraffin sections of 5-6 μm thickness were de-paraffinized with xylene. Rehydration was performed by placing sections in two changes of 100% alcohol for 10 minutes each, followed by descending grades of alcohol (two changes of 95% alcohol 10 minutes each). For complete rehydration, sections were washed in two changes of distilled water for five minutes each. Tissue specimens were kept in 3% hydrogen peroxide for 10 minutes to block the activity of endogenous peroxidase. Tissue slides were then placed inside the microwave for 10 minutes in 0.01 M citrate buffer (pH 6.0) solution at the temperature of 65°C. Following the microwave, specimens were cooled down at room temperature and then rinsed three times with phosphate-buffered saline (PBS) for 5 minutes. Sections were incubated for 10 minutes with protein block to prevent non-specific reactions. The used primary antibodies were rabbit polyclonal anti-PCNA antibody (cross-reacts with rat) (abx013174, Abbeva, United Kingdom at a dilution of 1:100), a marker of cell proliferation, rabbit polyclonal anti-caspase-3 antibody, (cross-reacts with rat) (A11319, ABclonal, USA at a dilution of 1:100), a marker of cell apoptosis and the monoclonal mouse anti-human antibody, (M7082, Dako, Singapore at a dilution of 1:50) for CD44 which was used to confirm MSCs. These antibodies were kept at 4°C overnight. PCNA, Caspase 3, and CD44 were performed on a DakoCytomation AutoStainer. Following washing three times by PBS for 5 minutes, the slides were incubated with biotinylated secondary antibody for 30 minutes at room temperature. Sections were washed four times in the buffer for five minutes each. Two to three drops of HRP-conjugated streptavidin enzyme label were placed on each

slide. The slides were incubated for 45 minutes at room temperature in the humidity chamber. Sections were washed four times in the buffer for five minutes each. Following that, slides were incubated with DAB (Diaminobenzidine) for 3 minutes. Later counterstaining was performed using Harry's hematoxylin. Results were interpreted using a light microscope.

Preparation of Bone-Marrow-Derived MSCs

Bone-marrow-derived MSCs were created by flushing the tibiae and femurs of 6-week-old male white albino rats with Dulbecco's changed Eagle's medium enhanced with 10% fetal bovine serum. The bone marrow was extracted. Nucleated cells were separated, aided by a density gradient, and re-suspended in a full culture medium with 1% penicillin-streptomycin. As a primary culture or after the development of substantial colonies, cells were incubated for 7 days at 37 °C in 5% humidified CO₂. After two PBS washes, cultures were trypsinized with 0.25% trypsin in 1 mM EDTA for five minutes at 37 °C once sizable colonies had formed (80–90% confluence). Centrifugation was followed by resuspension of the cells in media containing serum and incubation in 50- cm² culture flasks (Falcon). First-passage cultures was the term given to the resulting cultures. Additionally, we identified CD90 and CD34 as MSC surface markers using flow cytometry.

Ethical Approval

The study's goals were reviewed by the staff in charge. The Ethics Committee of the Faculty of Medicine Aswan University revised and approved this work. The protocols for animal experimentation and handling of animals followed the ethical standards laid down in The Helsinki Declaration, the Animal Welfare Act, and the Guide for the Care and the Use of Laboratory Animals.

Image analysis

Aided by a computer, digital picture analysis (Digital morphometric study)/ Slide digitization and imaging:

With a 0.5X photo adaptor attached to an Olympus microscope and a 40X objective, slides were

photographed and saved as TIFF files. Using VideoTest Morphology® software (Russia), which has a dedicated built-in routine for area measurement, cell counting, and stain measurement, the results photos were examined on an Intel® Core i7® based computer.

Five random fields from each of the two slides created for each scenario were examined.

Statistical analysis

Statistical Package for social science (SPSS) version 26.0 was used to tabulate, code, and analyze data to provide descriptive data. Data were expressed as Mean \pm SD. One way ANOVA (Analysis of variance) was used to compare between over two different groups of numerical (parametric) data followed by post-hoc Tukey. P value <0.05 was considered statistically significant.

RESULTS

Haematoxylin and eosin staining

Haematoxylin and eosin staining of the control group revealed the presence of well-defined cut sections of proximal convoluted tubules lined by cubical cells with basal rounded nuclei and a striated border on their lumen (many microvilli). As for distal convoluted tubules, there were well-defined cut sections lined by low cubical cells. Visceral and parietal layers of Bowman's space were well visualized with patent Bowman's space. All examined glomeruli were normal (Fig. 1A). The cisplatin-treated group (group II) had a dilated tubular system with thinned lining cells of proximal and distal convoluted tubules, cloudy swelling of the tubular system, narrow lumens of proximal convoluted tubules, some darkly stained nuclei, and marked cytoplasmic vacuolation in the cytoplasm of collecting ducts, as well as presence of inflammatory cells in the interstitium (Fig. 1B). When cisplatin and bone marrow stem cells were co-administered (group III), hematoxylin and eosin staining revealed well-defined cut sections of proximal and distal convoluted tubules lined by cubical cells with basal rounded nuclei, their lumen showed striated border (many microvilli), visceral and parietal layers of Bowman's space were well visualized, and all glomeruli had nor-

mal appearance (Fig. 1C). After one month of cisplatin administration without further intervention (group IV), hematoxylin and eosin staining showed dilated tubular system with thinned lining cells. Bowman's space was significantly dilated and the interstitium was noticeably infiltrated with inflammatory cells (Fig. 1D).

Masson trichrome staining

In the control group (group I), Masson trichrome staining revealed well-defined cut sections of the tubular system, patent Bowman's space with normal width. All glomeruli had normal configuration, and a small amount of collagen was seen. Within 8 days of cisplatin injection (group II), Masson trichrome staining revealed significantly increased amount of collagen in the interstitium (Fig. 2A). When the rats were co-treated with cisplatin and bone marrow stem cells (group III), the interstitium showed little amount of collagen compared to cisplatin only-injected rats (Fig. 2B). After one month of cisplatin injection with no further administrations (group IV), staining with Masson trichrome showed significantly increased collagen levels in the interstitium (Fig. 2C). There were statistically significant differences between the studied groups in the percent of Masson area with the highest mean values in the cisplatin group and lowest mean values in the control group with in-between significant differences, as the stem cell group showed significantly lower mean values than the cisplatin group but higher than the control group. After 30 days of cisplatin injection, the percentage of Masson area was lower than in the cisplatin group but higher than in the control group or stem cell group, with statistically significant differences (Table 1).

Immunohistochemistry

The lining tubular epithelial cells for the group that received cisplatin on the eighth day showed some positive PCNA immunoreactive nuclei (Fig. 3A), in contrast to the immunodetection of PCNA in the control group, which showed typical renal parenchyma with focal positive PCNA cells. Thirty days after cisplatin administration (withdrawal group), the lining tubular epithelial cells' PCNA staining indicated many positive PCNA im-

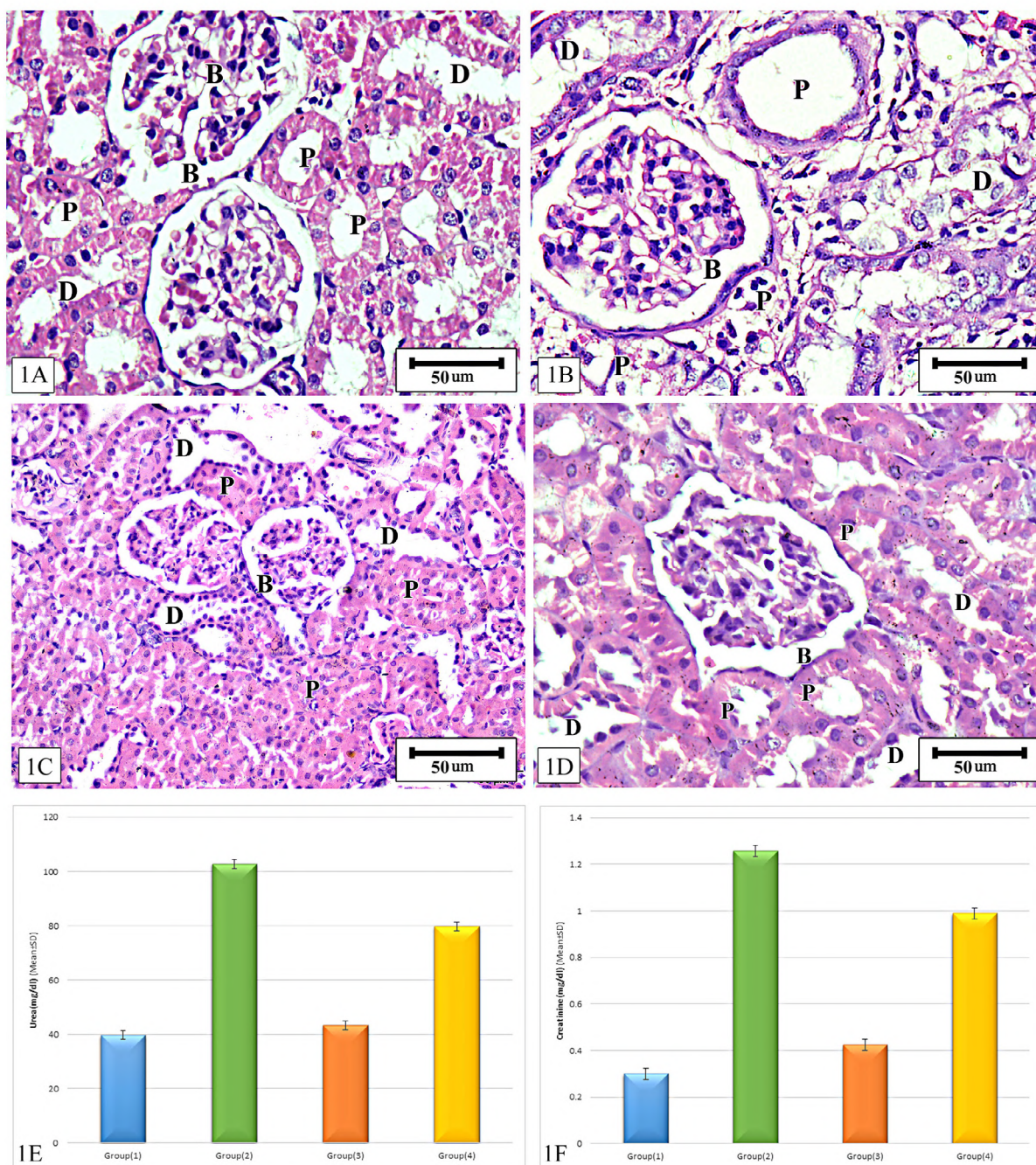


Fig. 1.- Histopathological analysis. The kidney sections were stained with hematoxylin and eosin, and representative images are shown. **(A)** The control group showed normal renal parenchyma. **(B)** The cisplatin-treated group exhibited dilated tubular system with thinning of lining cells of proximal and distal convoluted tubules, cloudy swelling of tubules, a narrow lumen of proximal convoluted tubules, some nuclei are darkly stained, the cytoplasm of collecting ducts showed marked cytoplasmic vacuolation, inflammatory cells in the interstitium. **(C)** The MSC group showed tubules less dilated, well-defined cut sections of proximal and distal convoluted tubules lined by cubical cells with basal rounded nuclei, their lumen shows striated border (many microvilli), well-visualized visceral and parietal layers of Bowman's space. **(D)** The withdrawal group revealed a less dilated tubular system with thinning of lining cells, the interstitium is infiltrated with inflammatory cells. **(E)** Mean \pm SD of blood urea (mg/dl) levels between the studied groups. **(F)** Mean \pm SD of serum creatinine (mg/dl) levels between the studied groups. Proximal convoluted tubules (P), Distal convoluted tubules (D), Bowman's space (B). Scale bars (A-D): 50 μ m.

munoreactive nuclei (Fig. 3C), suggesting that a self-repair system may be triggered in the injured kidneys. Comparing the stem cell group to other groups, positive PCNA immunoreactive nuclei seemed more common (Fig. 3B). There were sta-

tistically significant differences in the number of nuclei stained by PCNA among the studied groups, with the highest mean values among the stem cells group and the lowest mean values among the control group, and with in-between statistical-

ly significant differences as the withdrawal group had higher mean values of nuclei stained by PCNA than cisplatin group (Table 1).

Caspase 3

The kidneys of rats in control groups showed normal renal parenchyma with focal positive cytoplasmic Caspase-3 protease activity by immunodetection of caspase 3. The Caspase-3 protease activity in cisplatin-rat kidneys (group II) increased gradually over time relative to the controls at all periods (Fig. 4A), becoming statistically significant by day 30 (withdrawal group) (Fig. 4C). We discovered, however, that administration of MSCs during cisplatin-induced AKI dramatically reduced kidney caspase-3 levels (Fig. 4B). There were statistically significant differences between the studied groups in the intensity of Caspase-3, with the highest mean values among rats in the withdrawal group and the lowest mean values in

the control group, and with in-between statistically significant differences as Caspase-3 intensity was higher among the cisplatin group than stem cell group (Table 1).

Cluster of differentiation (CD44)

Our findings showed that CD44 was found in stem cells of rats near the tubules (Fig. 5C), confirming the localization of the BMMSCs in the tubules in the cortex, and repairing the tubular cells of injured kidneys. Immunodetection of CD44 for the control group revealed some positive CD44 (Fig. 5A). Statistically significant differences were reported between the studied groups regarding the number of CD44 cells, with the highest mean values in the stem cell group (group III) and lowest mean values in the control group, and with significantly higher mean values in the withdrawal group than in the cisplatin-treated group (Table 1).

Table 1. Comparison of Masson trichrome stain surface area, PCNA (No. of nuclei/H.P.F.), Caspase 3 (Intensity), CD44 (No. of stem cells/H.P.F.), Urea (mg/dl) and s. creatinine (mg/dl) between the studied groups.

	Group (I)	Group (II)	Group (III)	Group (IV)	P value
Masson % area	3.07±0.94	15.98±2.25	8.92±1.44	12.45±1.74	<0.001*
Post-hoc		P1=<0.001*	P1=<0.001* P2=<0.001*	P1=<0.001* P2=<0.001* P3=<0.001*	
PCNA (No. of nuclei/HPF)	8.55±2.46	35.97±8.68	162.70±16.86	95.10±11.84	<0.001*
Post-hoc		P1=<0.001*	P1=<0.001* P2=<0.001*	P1=<0.001* P2=<0.001* P3=<0.001*	
Caspase 3 (Intensity)	419.0±56.25	1800.0±240.80	947.40±88.14	2683.0±32.04	<0.001*
Post-hoc		P1=<0.001*	P1=<0.001* P2=<0.001*	P1=<0.001* P2=<0.001* P3=<0.001*	
CD44 (No. of S C/HPF)	6.98±2.18	12.13±3.63	44.70±12.18	30.42±9.48	<0.001*
Post-hoc		P1=0.006*	P1=<0.001* P2=<0.001*	P1=<0.001* P2=<0.001* P3=<0.001*	
Urea(mg/dl)	39.66±1.63	102.80±4.19	43.39±3.65	79.84±5.73	<0.001*
Post-hoc		P1=<0.001*	P1=0.4 P2=<0.001*	P1=<0.001* P2=<0.001* P3=<0.001*	
S.creatinine (mg/dl)	0.300±0.024	1.257±0.080	0.425±0.039	0.990±0.119	<0.001*
Post-hoc		P1=<0.001*	P1=0.04* P2=<0.001*	P1=<0.001* P2=<0.001* P3=<0.001*	

Data expressed as Mean ± SD

SD: standard deviation

P: Probability *:significance <0.05

Test used: One way ANOVA followed by post-hoc Tukey

P1: significance vs Group (1), P2: significance vs Group (2), P3: significance vs Group (3).

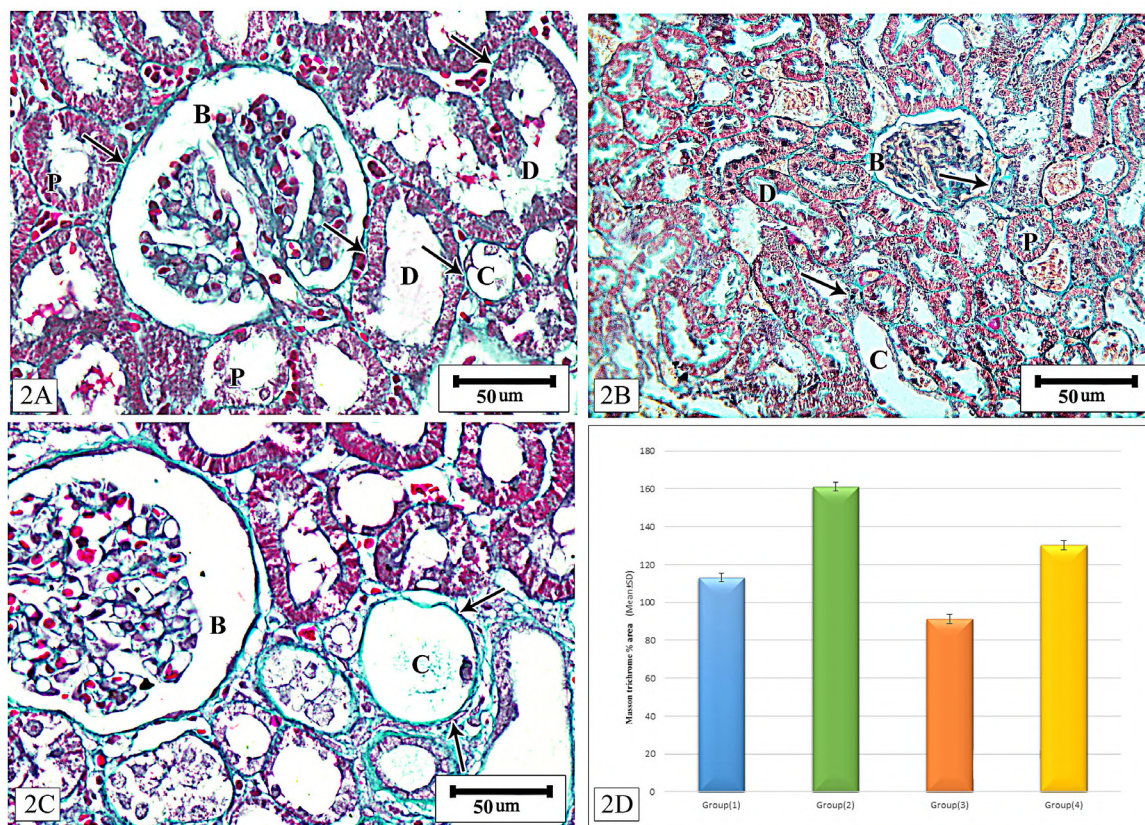


Fig. 2.- (A) The cisplatin-treated group (group II), Masson trichrome staining revealed an increase in the amount of collagen in the interstitium (arrows). (B) The cisplatin and bone marrow stem cells had little collagen in the interstitium. (arrows). (C) Staining with Masson trichrome for the withdrawal group (group IV) increased collagen levels in the interstitium (arrows). (D) Mean±SD of Masson trichrome % area between the studied groups. Proximal convoluted tubules (P), Distal convoluted tubules (D), Bowman's space (B). Collecting tubules (C). Scale bars (A-C): 50 µm.

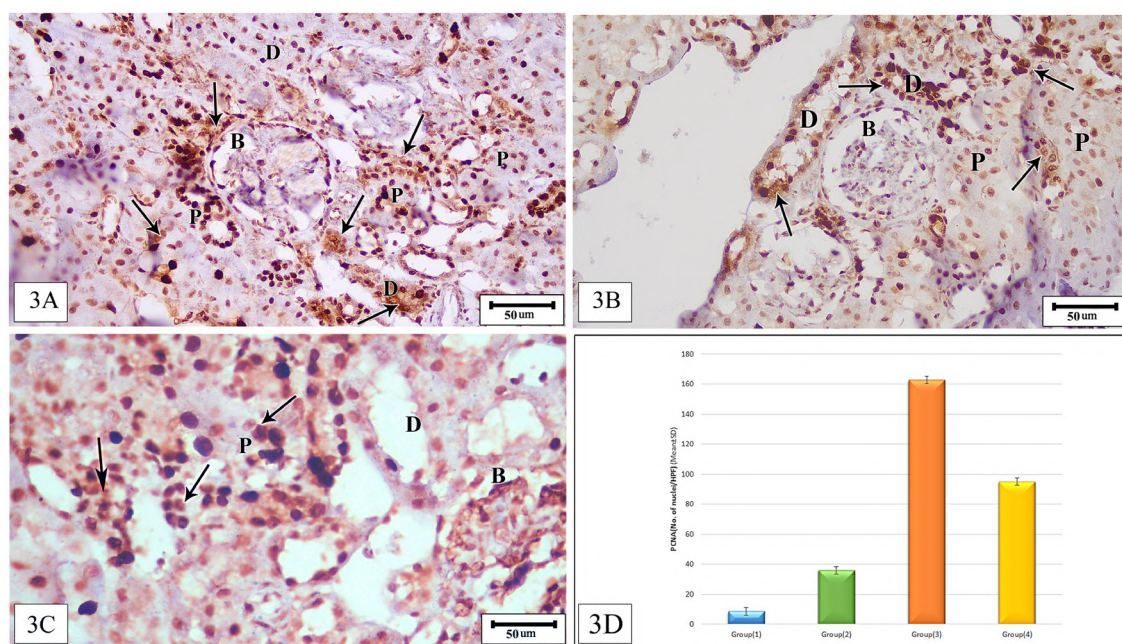


Fig. 3.- Immunodetection of PCNA: (A) PCNA staining for the cisplatin-treated group at day eight revealed some PCNA immunoreactive nuclei in the lining tubular epithelial cells (arrows). (B) PCNA staining for the cisplatin and bone marrow stem cells group revealed an apparent increase in positive PCNA immunoreactive nuclei in contrast to other groups (arrows). (C) The lining tubular epithelial cells for the withdrawal group displayed many positive PCNA immunoreactive nuclei (arrows). (D) Mean ± SD deviation of PCNA (No. of nuclei/HPF) between the groups under study. Proximal convoluted tubules (P), Distal convoluted tubules (D), Bowman's space (B). Scale bars (A-C): 50 µm.

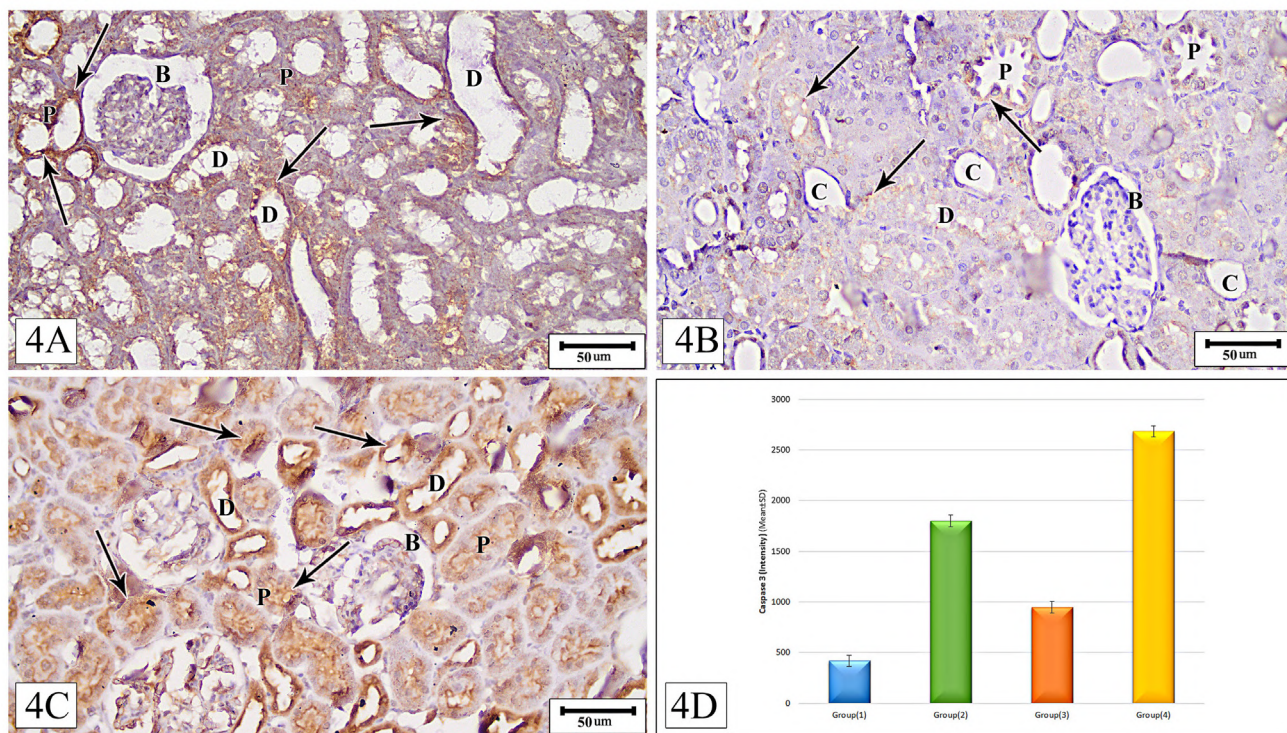


Fig. 4.- Immunodetection of caspase 3: (A) a cisplatin-treated rat (group II) showing positive expression of caspase-3 protease activity (arrows). (B) cisplatin and bone marrow stem cells group showed decreased expression of caspase-3 protease activity (arrows). (C) withdrawal group showed increased expression of caspase-3 protease activity (arrows). (D) Mean \pm SD of Caspase 3 (Intensity) between the studied groups. Proximal convoluted tubules (P), Distal convoluted tubules (D), Bowman's space (B), Collecting tubules (C). Scale bars (A-C): 50 μ m.

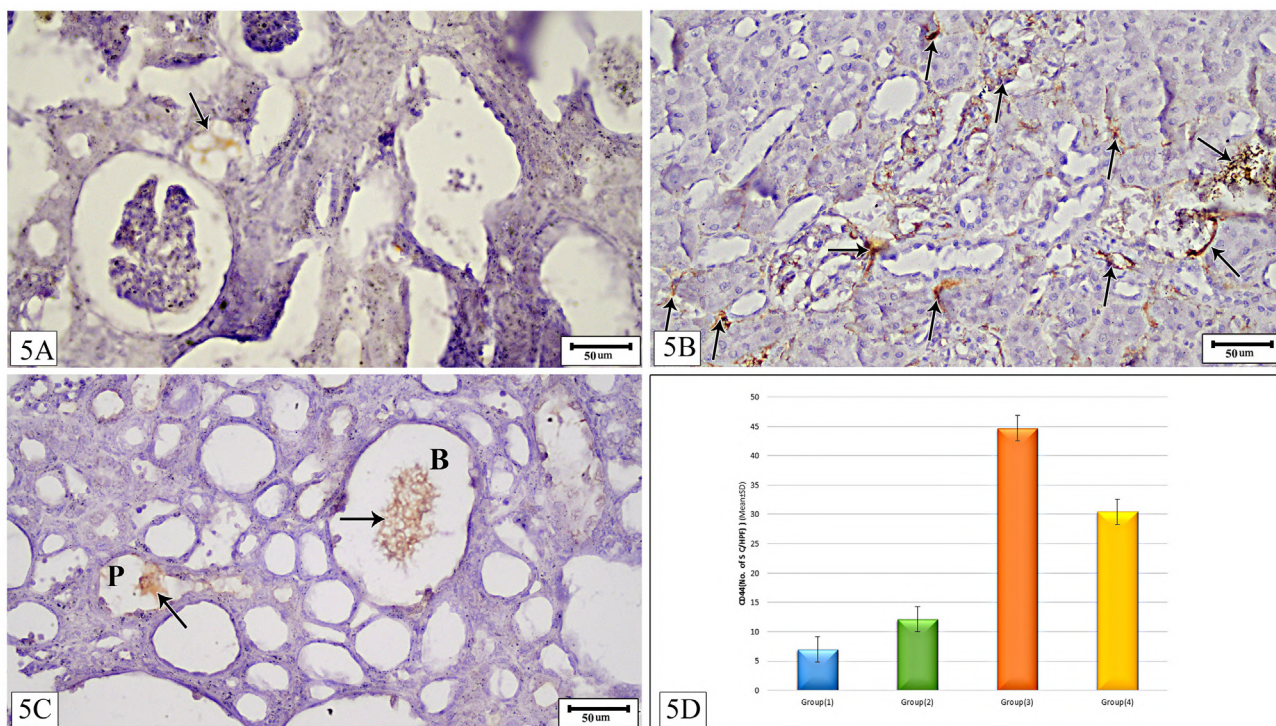


Fig. 5.- Immunodetection of CD44: (A) a control rat showing expression of CD44 (arrow). (B) cisplatin-treated group showed expression of CD44 (arrows). (C) MSCs group showed increased expression of CD44 (arrows). (D) Mean \pm SD of CD44 (Number of stem cells/H.P.F.) between the studied groups. Proximal convoluted tubules (P), Bowman's space (B). Scale bars (A-C): 50 μ m.

Biochemical reaction: Our results demonstrated a statistically significant difference in blood urea and serum creatinine levels between the studied groups, with rats receiving cisplatin having the highest mean values and rats in the control group having the lowest mean values, with similar outcomes between the stem cells group and control group (Table 1).

DISCUSSION

Acute kidney injury (AKI) is characterized by an abrupt drop in glomerular filtration rate, the kidney's inability to eliminate waste products such as nitrogen wastes, and disruptions in the homeostasis of fluids and electrolytes. Drug-induced nephrotoxicity, when the predominant site of the lesion is the proximal convoluted tubules of the nephron, is one of the renal or intrinsic causes of AKI (Makris and Spanou, 2016). Recent advances in cell therapy have shown positive therapeutic outcomes for kidney damage (KI). However, more research on the effects of genetic and biomolecular factors is required before contemplating the use of this therapy as a medical alternative. BMSCs and in-vitro-grown mesenchymal stem cells were the main subjects of the majority of these investigations (Zhou et al., 2020). Our findings showed that a statistically significant difference existed between the test groups regarding blood urea and serum creatinine levels as rats received cisplatin had the highest mean values, while rats in the control group had the lowest mean values with comparable results between stem cells group and the control group, demonstrating a striking increase in creatinine in cisplatin-treated group. At day 30 post-AKI, however, a decrement was observed in withdrawal and stem cell groups. Even though there was no statistically significant difference between the control and stem cell groups, this could be explained by the initial restoration of renal function. Similarly to this, Takai et al. (2015) reported that mice given CDDP (30 mg/kg) had blood creatinine concentrations of $(1.72 \pm 0.37 \text{ mg/dl})$ 24 hours later. According to histopathological examination, CDDP causes acute tubular necrosis (ATN), per the World Health Organization's categorization of tubulointerstitial disorders, which takes into account the etiology, clinical, and histological characteristics.

In our study, inflammatory infiltration and tubular dilatation, both histological features associated with toxic ATN were seen in the cisplatin-treated group. These outcomes are in agreement with Takai et al. (2015), who studied mice kidneys obtained 72 hours after CDDP injection and reported tubular necrosis, dilatation, and hyaline casts. Our findings in the cisplatin-treated and withdrawal groups at days 8 and 30 post-AKI were in line with (Fogo and Kashgarian, 2017), who found a dilated tubular system and inflammatory infiltration.

Our findings corroborated those of Liu et al. (2016), who administered 20 mg/kg of CDDP in mice intraperitoneally and reported severe pathological changes characterized by distortion of the overall kidney morphology, particularly dilation of renal tubules. Mata-Miranda et al. (2019), administered 15 mg/kg of CDDP intraperitoneally in mice and reported similar results 4 days after AKI.

In the MSCs group, the tubules were less dilated and the microarchitecture was better retained. The proximal tubular cells also contained cytoplasmic vacuoles. It is known that cells with reversible lesions can be identified under a microscope by the presence of hazy swelling or hydropic degeneration, which is brought on by ions and fluid homeostasis, and results in an increase of intracellular water. These findings imply that the degenerative process of nephrotoxicity was prevented in the early stages in the treated mice, encouraging a regeneration process that is consistent with Elseweidy et al. (2017), Begum et al. (2019) and Mata-Miranda et al. (2019). It has been demonstrated in several studies using mice models of acute renal failure (ARF) that MSCs can localize in injured kidneys, promoting both morphological and functional recovery (Herrera et al., 2007; Mata-Miranda et al., 2019). It is interesting to note that PCNA participates in DNA repair and its expression promotes the recovery of injured cells as well as mitogenesis and the replacement of damaged epithelial cells (Choe and Moldovan, 2017). Proliferating cell nuclear antigen (PCNA) expression levels rising in renal cells may be related to the progression of renal disease, and markers of renal cell activation and proliferation, such as immunostaining of renal tissue for PCNA. This

may be helpful in the diagnosis and/or prognosis of renal diseases (Pramanik et al., 2019). According to our findings, the tubular epithelial cells on the eighth day after cisplatin therapy revealed a few positive PCNA immunoreactive nuclei. In the tubular epithelial cells (withdrawal group), PCNA staining revealed several positive PCNA immunoreactive nuclei, indicating that a self-repair system may be triggered in the injured kidneys. Comparing the stem cell group to other groups, there was an apparent increase in PCNA immunoreactive nuclei that were positive. These findings showed that MSCs might restore AKI-damaged kidneys by preventing apoptosis and encouraging tubular cell growth. MSCs support regeneration and inhibit apoptosis in cisplatin-induced nephrotoxicity. Caspases (cysteine proteases) function upstream of DNA fragmentation and are crucial for both the execution of apoptotic cell death and its modulation (Yuan et al., 2016). Our findings demonstrated that the Caspase-3 protease activity in treated rat kidneys increased gradually over time relative to the controls at all periods, becoming statistically significant by day 30 (withdrawal group). However, we discovered that the administration of MSCs during cisplatin-induced AKI dramatically reduced kidney Caspase-3 levels. Our findings revealed that the nephroprotective impact of MSCs during cisplatin-associated AKI was partially mediated by Caspase-3 activation. These outcomes are supported by Ying et al. (2020). These results imply that cisplatin nephrotoxicity may be prevented and treated effectively by inhibiting apoptosis as a therapeutic approach. According to our findings, MSCs prevent kidney apoptosis in AKI as seen by decreased Caspase-3 expression. Glomerular parietal epithelial cells in the adult kidney that are CD44-positive have recently been found to be the potential stem cells that might move within the glomerular tuft and tubules and differentiate into new cells (Herrera et al., 2007; Roeder et al., 2018). Glomerular parietal epithelial cells (GPECs), a group of cells lining the interior of Bowman's capsule, have been linked to CD44 expression (Hamatani et al., 2020). It has been demonstrated that GPECs move into the glomerular tuft and develop into mature podocytes (Miesen et al., 2017). Additionally, a subgroup of GPECs in the adult human kidney's Bowman's capsule exhib-

it characteristics of multipotent progenitor cells and take part in renal healing (Huang et al., 2021). CD44 may help promote renal regeneration by attracting exogenous MSC to damaged renal tissue (Herrera et al., 2007; Liesveld et al., 2020). Studies suggest that stimulation of the receptor by its ligand stromal-derived factor may play a significant role in the migration of transplanted MSC to areas of injury in the ovary (Ling et al., 2022). Although CXCR4 appears to be expressed at a low level on the surface of MSCs, studies suggest that this receptor may be stimulated by its ligand (Wynn et al., 2004). Our results showed that CD44 was detected in many cells around the tubules in stem cell of rats, which verify the localization of the BMMSCs in the tubules in the cortex, repairing the tubular cells of injured kidneys. These results came in agreement with Herrera et al. (2007), who demonstrated that the localization of exogenous MSC to damaged renal tissue is influenced by the expression of cell surface CD44. Early MSC migration to the kidney, the functional and morphological healing of the injured kidney was hastened by the recruitment of MSCs (Herrera et al., 2007). However, Abd El Zaher et al. (2017), discovered that only a small proportion of bone-marrow-derived cells were integrated into the damaged tubules as epithelial cells. The degree of renal damage following an ischemia/reperfusion event determines whether bone-marrow-derived stem cells engraft into the tubules and take on an epithelial phenotype (Ornellas et al., 2017).

In conclusion, based on our preliminary research, it appeared that MSC reduces CDDP nephrotoxic damage, resulting in functional and histological repair. To suggest new preventative measures in nephrotoxic therapies and increase the possibilities for regenerative medicine, it is vital to research the protective processes and actions of the MSCs.

CONCLUSION

The MSC implant reduces the nephrotoxicity caused by cisplatin, which is reflected in functional and histological recovery. In conclusion, our early research revealed that MSCs reduce the nephrotoxic damage caused by cisplatin, resulting in functional and histological repair.

Recommendation: To suggest novel preventative measures in nephrotoxic therapies and increase the possibilities for regenerative medicine, it is vital to research the protective processes and actions of MSCs.

Data availability statement

This study was carried out in the Histology and Anatomy Departments, Faculty of Medicine, Assiut University. All data generated or analyzed during this study are included in this article, further inquiries can be directed to the corresponding author.

Authorship contribution: Author (A) collected the data and wrote the manuscript; Author (B) did histopathology; All work was under supervision of author (C). All authors contributed equally.

REFERENCES

- ABD EL ZAHER F, EL SHAWARBY A, HAMMOUDA G, BAHAA N (2017) Role of mesenchymal stem cells versus their conditioned medium on cisplatin-induced acute kidney injury in albino rat. A histological and immunohistochemical study. *Egypt J Histol*, 40(1): 37-51.
- ALY RM (2020) Current state of stem cell-based therapies: an overview. *Stem Cell Invest*, 7: 8.
- BEGUM S, AHMED N, MUBARAK M, MATEEN SM, KHALID N, RIZVI SAH (2019) Modulation of renal parenchyma in response to allogeneic adipose-derived mesenchymal stem cells transplantation in acute kidney injury. *Int J Stem Cells*, 12(1): 125-138.
- CHARMI A, BAHMANI M, SAJJADI M, KAZEMI R (2009) Morpho-histological study of kidney in farmed juvenile beluga, *Huso huso* (Linnaeus, 1758). *Pakistan J Biol Sci*, 12(1): 11-18.
- CHOE KN, MOLDOVAN G-L (2017) Forging ahead through darkness: PCNA, still the principal conductor at the replication fork. *Mol Cell*, 65(3): 380-392.
- DU T, ZOU X, CHENG J, WU S, ZHONG L, JU G, ZHU J, LIU G, ZHU Y, XIA S (2013) Human Wharton's jelly-derived mesenchymal stromal cells reduce renal fibrosis through induction of native and foreign hepatocyte growth factor synthesis in injured tubular epithelial cells. *Stem Cell Res Ther*, 4(3): 1-13.
- ELSEWEIDY M, ASKARM, ELSWEFY S, SHAWKY M (2018) Nephrotoxicity induced by cisplatin intake in experimental rats and therapeutic approach of using mesenchymal stem cells and spironolactone. *Appl Biochem Biotechnol*, 184(4): 1390-1403.
- FALL P, SZERLIP HM (2010) Continuous renal replacement therapy: cause and treatment of electrolyte complications. *Seminars in dialysis*, 23(6): 581-585.
- FOGO AB, KASHGARIAN M (2017) Diagnostic Atlas of Renal Pathology. 3rd ed. Philadelphia, Elsevier.
- HAMATANI H, ENG DG, HIROMURA K, PIPPIN JW, SHANKLAND SJ (2020) CD44 impacts glomerular parietal epithelial cell changes in the aged mouse kidney. *Physiol Rep*, 8(12): e14487.
- HERRERA M, BUSSOLATI B, BRUNO S, MORANDO L, MAURIELLO-ROMANAZZI G, SANAVIO F, STAMENKOVIC I, BIANCONE L, CAMUSSI G (2007) Exogenous mesenchymal stem cells localize to the kidney by means of CD44 following acute tubular injury. *Kidney Int*, 72(4): 430-441.
- HUANG J, KONG Y, XIE C, ZHOU L (2021) Stem/progenitor cell in kidney: characteristics, homing, coordination, and maintenance. *Stem Cell Res Ther*, 12(1): 1-18.
- LIESVELD JL, SHARMA N, ALJITAWI OS (2020) Stem cell homing: From physiology to therapeutics. *Stem Cells*, 38(10): 1241-1253.
- LING L, HOU J, LIU D, TANG D, ZHANG Y, ZENG Q, PAN H, FAN L (2022) Important role of the SDF-1/CXCR4 axis in the homing of systemically transplanted human amnion-derived mesenchymal stem cells (hAD-MSCs) to ovaries in rats with chemotherapy-induced premature ovarian insufficiency (POI). *Stem Cell Res Ther*, 13(1): 1-19.
- LIU M, JIA Z, SUN Y, ZHANG A, YANG T (2016) A H2S donor GYY4137 exacerbates cisplatin-induced nephrotoxicity in mice. *Mediators Inflamm*, 2016: 8145785.
- MAKRIS K, SPANOUL (2016) Acute kidney injury: definition, pathophysiology and clinical phenotypes. *Clin Biochem Rev*, 37(2): 85-98.
- MATA-MIRANDA MM, BERNAL-BARQUERO CE, MARTINEZ-CUAZITL A, GUERRERO-ROBLES CI, SANCHEZ-MONROY V, ROJAS-LOPEZ M, VAZQUEZ-ZAPIEN GJ (2019) Nephroprotective effect of embryonic stem cells reducing lipid peroxidation in kidney injury induced by cisplatin. *Oxid Med Cell Longev*, 2019: 5420624.
- MCSWEENEY KR, GADANEC LK, QARADAKHI T, ALI BA, ZULLI A, APOSTOLOPOULOS V (2021) Mechanisms of cisplatin-induced acute kidney injury: Pathological mechanisms, pharmacological interventions, and genetic mitigations. *Cancers (Basel)*, 13(7): 1572.
- MIESEN L, STEENBERGEN E, SMEETS B (2017) Parietal cells - new perspectives in glomerular disease. *Cell Tissue Res*, 369(1): 237-244.
- MILLER RP, TADAGAVADI RK, RAMESH G, REEVES W (2010) Mechanisms of cisplatin nephrotoxicity. *Toxins*, 2(11): 2490-2518.
- ORNELLASA FM, ORNELLASA DS, MARTINIA SV, CASTIGLIONE RC, VENTURA GM, ROCCO PR, GUTFILEN B, DE SOUZA SA, TAKIYA CM, MORALES MM (2017) Bone marrow-derived mononuclear cell therapy accelerates renal ischemia-reperfusion injury recovery by apoptotic related molecules. *Cell Physiol Biochem*, 41(5): 1736-1752.
- PRAMANIK S, SUR S, BANKURA B, PANDA CK, PAL D (2019) Expression of proliferating cell nuclear antigen and Ki-67 in renal cell carcinoma in eastern Indian patients. *Int Surg J*, 6(10): 3687-3693.
- ROEDER SS, BARNES TJ, LEE JS, KATO I, ENG DG, KAVERINA NV, SUNSERI MW, DANIEL C, AMANN K, PIPPIN JW, SHANKLAND SJ (2017) Activated ERK1/2 increases CD44 in glomerular parietal epithelial cells leading to matrix expansion. *Kidney Int*, 91(4): 896-913.
- SENBANJO LT, CHELLAIAH MA (2017) CD44: A multifunctional cell surface adhesion receptor is a regulator of progression and metastasis of cancer cells. *Front Cell Dev Biol*, (5): 18.
- TAKAI N, ABE K, TONOMURA M, IMAMOTO N, FUKUMOTO K, ITO M, MOMOSAKI S, FUJISAWA K, MORIMOTO K, TAKASU N, INOUE O (2015) Imaging of reactive oxygen species using [3H] hydromethidine in mice with cisplatin-induced nephrotoxicity. *EJNMMI Research*, 5(1): 1-8.
- ULLAH I, SUBBARAO RB, RHO GJ (2015) Human mesenchymal stem cells-current trends and future prospective. *Biosci Rep*, 35(2): e00191.
- WYNN RF, HART CA, CORRADI-PERINI C, EVANS CA, WRAITH JE, FAIRBAIRN LJ, BELLANTUONO I (2004) A small proportion of mesenchymal stem cells strongly expresses functionally active CXCR4 receptor capable of promoting migration to bone marrow. *Blood*, 104(9): 2643-2645.
- YING J, WU J, ZHANG Y, QIAN X, YANG Q, CHEN Y, ZHU H (2020) Ligustrazine suppresses renal NMDAR1 and caspase-3 expressions in a mouse model of sepsis-associated acute kidney injury. *Mol Cell Biochem*, 464(1): 73-81.
- YUAN J, NAJAFOV A, PY BF (2016) Roles of caspases in necrotic cell death. *Cell*, 167(7): 1693-1704.
- ZHOU S, QIAO YM, LIU YG, LIU D, HU JM, LIAO J, LI M, GUO Y, FAN LP, LI LY, ZHAO M (2020) Bone marrow derived mesenchymal stem cells pretreated with erythropoietin accelerate the repair of acute kidney injury. *Cell Biosci*, 10(1): 130.